around 275 nm and a small negative peak around 230 nm (Figure 9b). These are the typical features of B-form and A-form duplexes.[44,45] That is, N-gap DNA homoduplexes and RNA/DNA heteroduplexes used in this study should take the structures of B-form and A-form duplexes, respectively. One of the notable features of an A-form duplex is that the major groove is extremely narrow and very deep, while the minor groove is very broad and shallow.[46,47] This structure might explain the signal profile for RNA. **MNDS** protrudes its dansyl moiety to the major groove. A modeling study showed that the narrow and deep major groove of the heteroduplex does not leave space for β-CyD after the dansyl moiety sticks out (Figure 10a). Therefore, β-CyD could not

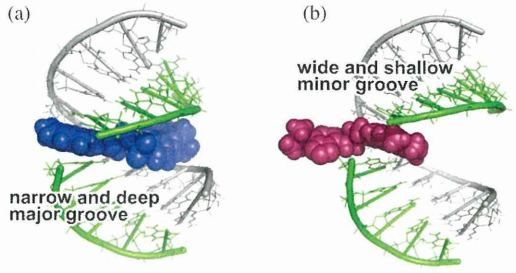

Figure 10. One of the possible 3D structures of a) **MNDS**/G-gap and b) **MNDB**/C-gap RNA/DNA heteroduplexes. The model was geometry-optimized by AMBER* force field with GB/SA (generalized Born/surface area) solvent model using MacroModel version 9.1. The fluorophore of **MNDS** is buried deeply in the major groove of the heteroduplex, while that of **MNDB** is exposed to the bulk solution from the shallow minor groove of the heteroduplex. The β-CyD moiety of the **CyD–ODN** was omitted from the structure for clarity.

access the dansyl moiety in the major groove of the heteroduplex, even from the 3′-end of **CyD–ODN**. The DBD moiety of **MNDB** protrudes into the minor groove. The DBD in the shallow minor groove seems to be accessible from both 3′- and 5′-ends of the **CyD–ODN**s, as shown in Figure 10b. Only the reporter ligands that protrude their signaling group into the minor groove could be used for RNA analysis.

Effect of temperature on the signal contrast: One of the merits of the present method is that the measurements for all of the targets using different DNA probes could be performed under the same conditions, because the recognition does not rely on subtle differences in thermal stabilities of the duplexes formed with the probes. Generally, DNA probing relies on the specificity of probe hybridization. Accordingly, to recognize one-base displacement, the temperature should be controlled in a narrow range between the melting temperatures of the full match and mismatch duplexes. In the present system, however, all the duplexes that interact with the reporter ligands are fully matched duplexes; only the unpaired base displayed in the gap is different. Therefore, the response is not completely independent of temperature, but the temperature range in which we can conduct the SNP assay should be quite wide compared with traditional probe hybridization. Fluorometric SNP analyses using **MNDS** and **3CyD–ODN**, for example, were performed to investigate an effect of the temperature on the signal contrast of this system. Normalized signals measured at different temperatures are shown in Figure 11 with the UV melting curve of the duplex. The signal quality (signal contrast) did not deteriorate much, even at 35 °C, which is below the

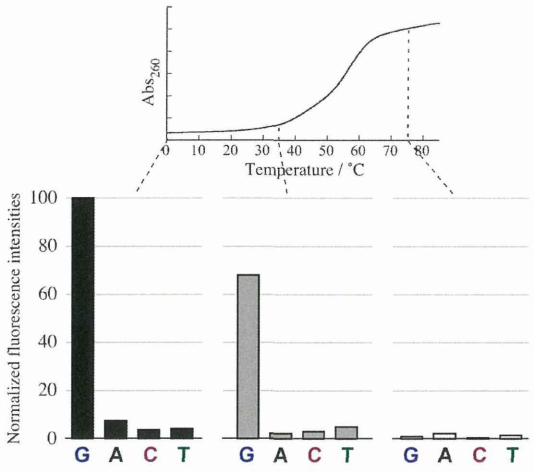

Figure 11. UV melting curve (top) and normalized fluorescence intensities (bottom) of **MNDS** in the presence of N-gap duplexes containing the **3CyD–ODN**. Fluorescence measurements were performed at 0 °C (left), 35 °C (center), and 75 °C (right). All other experimental conditions were the same as Figure 3.

melting temperature ($T_m \approx 50$ °C) of this duplex. The measurement at 75 °C was, of course, disabled. Thus, the assay can be carried out at any temperature that is lower than the T_m, because the duplex framework that provides the environment for nucleobase recognition/signaling is formed at temperatures below the T_m. The temperature dependence of the interaction of **MNDS** with G-gap DNA duplex also has to be taken into account. The decrease in the signal intensities at 35 °C compared with those at 0 °C observed in Figure 11 can be attributed to the temperature dependence of **MNDS** binding. As commonly observed in most bimolecular interactions, the bindings of MND and dansyl with the G-gap and β-CyD, respectively, are thought to weaken with a rise in temperature. However, the result showed that the temperature dependence of the **MNDS** binding was not so significant, at least in the temperature range of the present measurements. Even so, the measurement at 0 °C is the most desirable condition, which endorses a highest stabilization for all the duplexes in aqueous solutions. This unique feature (low temperature susceptibility) could be very important in massively parallel processing systems such as DNA arrays or chips.

Remaining problems and perspective: The general concerns for molecular probes are mainly selectivity and sensitivity.

To improve probes according to these two requirements, we have been conducting preliminary studies, separately, using various nucleobase-recognition ligands. For selectivity, we now have ligands that are complementary to each of the four nucleobases. For example, the C/T selectivity of naphthyridine can be controlled by introducing electron-withdrawing groups (such as a trifluoromethyl group) to the ring.[39] The protonation to the endocyclic nitrogens of naphthyridine is delocalized between the N1 and N8 positions. The electron-withdrawing effect seems to localize the protonation to the N1 position and makes the naphthyridine ring complementary to C. We have just reported that the C/T selectivity could also be controlled by competitive binding of additional ligands.[48] We have also published reports that alloxadine and lumazine have adenine selectivity.[38,49] All of these findings could be fed into the present system.

The sensitivity of the present system is adequate for the products of polymerase chain reactions (PCR), but still should be improved more for practical applications. Considering the properties of the fluorophores employed in this study, the signal intensities were supposed to be enhanced more than observed here. It was apparent that only a portion of the reporter ligands bound with the N-gaps under the experimental conditions. This is due to the low binding constant of the reporter ligands to the target N-gaps. If we use ligands with higher binding constants in this system, we could reduce the concentration of the ligand and, consequently, improve the signal contrast. We already succeeded in the synthesis of such ligands for some cases.[40] Alternatively or additionally, modification of β-CyD would be effective. For example, by making β-CyD hydrophobic (e.g., by methylation), both the binding constant and the fluorescence intensity of the inclusion complexes could be enhanced.[50]

Conclusions

A nucleobase-specific recognition system was constructed by the rational design of a combination between DNA/RNA-binding fluorescent reporter ligands and **CyD–ODN** conjugates. The two molecules work cooperatively to recognize/report specific nucleobases displayed in the gap of the duplexes. The groove in which the expected cooperation proceeds can be pre-assigned according simple rules. For DNA targeting, the signaling moiety located in the major groove interacts with the counterpart modified on the 3′-end of ODN, while the reporter moiety in the minor groove interacts with that on the 5′-end of ODN. The system permits the design of various reporting molecules in a logical manner. The reporting ligands could be prepared by covalently linking the selected recognition and fluorescent molecules through an alkyl chain, because the two elementary processes (recognition and reporting) are separated and allotted to two different sites on the duplex structure. Therefore, the two elementary functional groups can be chosen independently to design the desired reporting ligands for specific nucleobases and fluorescence colors.

The design of the proposed system is general; therefore, the signal is not be limited to fluorescence. Various signals (e.g., electrochemical, colorimetric, or catalytic) could be modulated by each of the specific counterparts through the controlled proximity in the major and minor grooves of the N-gap DNA duplexes.

Experimental Section

General: β-CyD and N-succinimidyl 3-(2-pyridyldithio) propionate (SPDP) were purchased from Sigma–Aldrich (Saint Louis, MO, USA) and Dojindo Laboratories (Kumamoto, Japan), respectively. RNA targets were purchased from Japan Bio Services (Saitama, Japan). All ODNs were synthesized by an automated DNA synthesizer (Expedite 8900) using conventional phosphoramidite methods. The phosphoramidite monomers were purchased from Proligo (Hamburg, Germany) and Glen Research (Sterling, VA, USA). After purification by HPLC, all ODNs and synthesized ODN conjugates were identified using MALDI-TOF mass spectrometry on a Bruker Daltonics Autoflex-III (Billerica, MA, USA). All other reagents were obtained as the highest grade and used without further purifications.

CyD–ODNs (**5CyD–ODNs** and **3CyD–ODNs**) were synthesized according to Scheme S1 (Supporting Information). 3′- or 5′-end aminopropyl-linked DNA was modified with a bifunctional linker molecule and then coupled with monothiolated **β-CyD**.

Synthesis of monotosylated β-CyD:[50] β-CyD (0.50 g, 0.43 mmol) was dissolved in dried pyridine (4.3 mL) under an atmosphere of argon. To the solution, *p*-toluene sulfonylchloride (0.16 g, 0.85 mmol) was added in an ice bath and then stirred at room temperature. The progress of the reaction was occasionally monitored by TLC (1-buthanol/ethanol/water = 5:4:3, indicator: *p*-anisaldehyde). The reaction was quenched by addition of water (0.35 mL) after 3 h. Analysis by TLC indicated the presence of the three spots corresponding to β-CyD (R_f = 0.30), monotosylated **β-CyD** (0.48), and ditosylated β-CyD (0.57) at almost the same density. The solution was concentrated to a half in vacuo and poured into acetone (8.5 mL) with vigorous stirring. The resulting white solid was collected and repeatedly recrystallized from water.

White solid 72 mg (12.7%); ^{1}H NMR (399.65 MHz, [D$_6$]DMSO): δ = 2.43 (s, 3H), 3.10–3.45 (m, 14H), 3.45–3.66 (m, 28H), 4.10–4.60 (m, 6H), 4.76 (s, br, 2H), 4.83 (s, br, 5H), 5.60–5.85 (m, 14H), 7.42 (d, 2H, J = 8.3 Hz), 7.74 ppm (d, 2H, J = 8.3 Hz).

Synthesis of monothiolated β-CyD:[51,52] Monotosylated **β-CyD** (0.50 g, 0.39 mmol) and thiourea (0.50 g, 6.6 mmol) were dissolved in aqueous methanol (25 mL, 80%) and refluxed for 72 h. The solution was evaporated in vacuo. The solid was suspended in methanol (7.6 mL) and stirred for 1 h at room temperature. The solid was filtered and dissolved in aqueous solution of NaOH (17 mL, 10%) and stirred for 5 h at 50 °C. After the solution was acidified with HCl (1 M) to pH 2, trichloroethylene (1.2 mL) was added. After stirring overnight, the precipitate was filtered and washed with water. Evaporation of trichloroethylene in vacuo followed by repeated recrystallization from water gave a white solid.

White solid 0.27 g (59.4%); TLC (silica), one spot, R_f = 0.23 (CH_3CO_2Et/*n*-PrOH/H_2O, 7:7:5); MS (MALDI-TOF): m/z calcd for $[M+H]^+$: 1150.54; found: 1150.06.

Synthesis of SPDP–DNA conjugate: The purified 3′- or 5′-end aminopropyl-linked ODN (100 nmol) was dissolved in carbonate Na buffer (100 μL, 0.5 M, pH 9.3). To this solution, SPDP (1.5 mg, 4.6 μmol) dissolved in DMSO (50 μL) was added. The resulting suspension was stirred at ambient temperature overnight. The solution was diluted to 400 μL with water. The mixture was purified by RP-HPLC under the following conditions. Column: Wakosil-II 5C18 RS, room temperature, flow rate: 1.0 mL min^{-1}, eluent A: TEAA (triethylamine–acetic acid, 0.1 M, pH 7.0),

eluent B: acetonitrile, linear gradient: 5–30% B in 30 min, detection wavelength: 260 nm.

MS (MALDI-TOF): *m/z* calcd for $[M-H]^-$ (3′-modified): 2746.46; found: 2746.81; *m/z* calcd for $[M-H]^-$ (5′-modified): 2724.50; found: 2724.37.

Synthesis of β-CyD–DNA conjugate (CyD–ODN): **SPDP–DNA** conjugate (50 nmol) was dissolved in phosphate–Na buffer (100 μL, 10 mM, pH 7.2). To this solution was added monothiolated **β-CyD** (5.8 mg, 5.0 μmol) dissolved in DMSO (60 μL). The resulting suspension was stirred at ambient temperature overnight. The solution was diluted to 400 μL with water. The mixture was purified by RP-HPLC under the following conditions. Column: Wakosil-II 5C18 RS, room temperature, flow rate: 1.0 mL min^{-1}, eluent A: 0.1 M TEAA (pH 7.0), eluent B: acetonitrile, linear gradient: 5–30% B in 30 min, detection wavelength: 260 nm.

MS (MALDI-TOF): *m/z* calcd for $[M-H]^-$ (3′-modified): 3771.77; found: 3770.94; *m/z* calcd for $[M-H]^-$ (5′-modified): 3749.81; found: 3748.90.

Synthesis of MNDS: **MNDS** was synthesized as described previously.[36] The outline of the procedure is as follows. Aminonaphthyridine was coupled with activated ester of N-protected aminopropionate to form a naphthyridine connected with a protected aminolinker chain through an amide bond. After deprotection, it was coupled with dansyl chloride to obtain **MNDS**.

Synthesis of MNDB: **MNDB** was synthesized as described previously.[53] The outline of the procedure is as follows. Aminonaphthyridine was chlorinated and then coupled with 1,2-diaminoethane to form a naphthyridine derivative with an aminolinker chain, which is tethered through the secondary amine. Finally, it was coupled with DBD-F (7-fluoro-4-(*N*,*N*-dimethylaminosulfonyl)benzofurazan) to obtain **MNDB**.

Synthesis of 3,5-diamino-*N*-(2-((2-aminoethyl)amino)ethyl)-6-chloropyrazine-2-carboxamide:[54] Methyl-3,5-diamino-6-chloropyrazine-2-carboxylate (1.0 g, 4.9 mmol) was added to diethylenetriamine (1.5 g, 15 mmol) and stirred for 24 h at 100 °C. The solution was suspended in $CHCl_3$ and subsequently extracted with HCl (0.1 M). The aqueous layer was neutralized with NaOH and extracted with $CHCl_3$. The organic layer was concentrated in vacuo and the crude residue was purified by column chromatography on amino-group-modified silica gel ($CHCl_3$/MeOH). The obtained residue was identified by MALDI-TOF MS and was used for the next step without further purification.

Synthesis of DPDB: To a mixture of 3,5-diamino-*N*-(2-((2-aminoethyl)amino)ethyl)-6-chloropyrazine-2-carboxamide (50 mg, 0.21 mmol) and DBD-F (70 mg, 0.31 mmol) in DMF (8 mL), triethylamine (4 mL) was added and the reaction mixture was stirred and refluxed under N_2 atmosphere for 12 h. The solvent was concentrated in vacuo and the crude product was purified by column chromatography on an amino-group-modified silica gel ($CHCl_3$/MeOH).

Yellow solid 29 mg (28%); ^{1}H NMR (400 MHz, DMSO): $\delta = 7.87$ (d, 1H, $J = 7.5$ Hz), 7.51 (br, 1H), 6.85 (br, 1H), 6.09 (d, 1H, $J = 7.5$ Hz), 5.11 (s, 2H), 3.51 (m, 2H), 3.42 (m, 2H), 3.08 (m, 2H), 2.87 (m, 2H), 2.85 ppm (s, 6H); MS (ESI): *m/z* calcd for $C_{17}H_{24}ClN_{10}O_4S$: 499.1391 $[M+H]^+$; found: 499.1386.

Circular dichroism (CD) measurements: CD spectra were obtained using a JASCO J-725 spectropolarimeter equipped with a Peltier thermal controller. CD spectra were measured from 360 to 200 nm in a 0.1 cm path length cell at 0 °C during N_2 purging to prevent moisture condensation on the cell. The concentration of the samples was 1.25 μM in 10 mM phosphate buffer (pH 7.0) containing NaCl (1 M).

Fluorescence measurements: Fluorescence measurements were performed at 0 °C using a JASCO FP-6500 spectrofluorometer and a PerkinElmer LS55 equipped with a Peltier thermal controller during N_2 purging to prevent moisture condensation on the quartz cell. Each of the reporter molecules (5.0 μM) was added into the solution of N-gap duplexes (1.0 μM) dissolved in phosphate buffer (10 mM, pH 7.0), NaCl (1 M), and DMSO (0.83%), and subjected to a measurement. Normalized fluorescence intensities were estimated after subtraction of the signal of the reporter molecule alone from each measurement.

Acknowledgements

We thank Ms. M. Miyabe for assistance in the mass spectrometry measurements for **CyD–ODN** conjugate identification. We also thank Prof. H. Ihara and Dr. H. Jintoku for their support in measuring CD and fluorescence spectra. This work was supported by the Grant-in-Aid for Scientific Research on Innovative Areas (Coordination Programming, Area 2107) [No. 24108734 to T.I.], Scientific Research (B) [No. 24350040 to T.I.] from the Ministry of Education, Culture, Sports, Science and Technology, Japan; and the Health Labour Sciences Research Grant (Research on Publicly Essential Drugs and Medical Devices) [to T.I.] from the Ministry of Health and Labour, Japan.

[1] D. M. Kolpashchikov, *Chem. Rev.* **2010**, *110*, 4709–4723.
[2] A. B. Iliuk, L. Hu, W. A. Tao, *Anal. Chem.* **2011**, *83*, 4440–4452.
[3] J. Liu, Z. Cao, Y. Lu, *Chem. Rev.* **2009**, *109*, 1948–1998.
[4] A. C. Syvänen, *Nat. Rev. Genet.* **2001**, *2*, 930–942.
[5] V. Lyamichev, A. L. Mast, J. G. Hall, J. R. Prudent, M. W. Kaiser, T. Takova, R. W. Kwiatkowski, T. J. Sander, M. de Arruda, D. A. Arco, B. P. Neri, M. A. D. Brow, *Nat. Biotechnol.* **1999**, *17*, 292–296.
[6] S. Tyagi, F. R. Kramer, *Nat. Biotechnol.* **1996**, *14*, 303–308.
[7] B. Dubertret, M. Calame, A. J. Libchaber, *Nat. Biotechnol.* **2001**, *19*, 365–370.
[8] H. Kashida, T. Takatsu, T. Fujii, K. Sekiguchi, X. Liang, K. Niwa, T. Takase, Y. Yoshida, H. Asanuma, *Angew. Chem.* **2009**, *121*, 7178–7181; *Angew. Chem. Int. Ed.* **2009**, *48*, 7044–7047.
[9] T. Ihara, M. Mukae, *Anal. Sci.* **2007**, *23*, 625–629.
[10] Y. N. Teo, E. T. Kool, *Chem. Rev.* **2012**, *112*, 4221–4245.
[11] J. D. Wulfkuhle, L. A. Liotta, E. F. Petricoin, *Nat. Rev. Cancer* **2003**, *3*, 267–275.
[12] Y. Urano, *Anal. Sci.* **2008**, *24*, 51–53.
[13] J. Li, W. Zhou, X. Ouyang, H. Yu, R. Yang, W. Tan, J. Yuan, *Anal. Chem.* **2011**, *83*, 1356–1362.
[14] D. C. Harris, B. R. Saks, J. Jayawickramarajah, *J. Am. Chem. Soc.* **2011**, *133*, 7676–7679.
[15] K. Gorska, A. Manicardi, S. Barluenga, N. Winssinger, *Chem. Commun.* **2011**, *47*, 4364–4366.
[16] Y. Sato, S. Nishizawa, K. Yoshimoto, T. Seino, T. Ichihashi, K. Morita, N. Teramae, *Nucleic Acids Res.* **2009**, *37*, 1411–1422.
[17] Y. Sato, T. Ichihashi, S. Nishizawa, N. Teramae, *Angew. Chem.* **2012**, *124*, 6475–6478; *Angew. Chem. Int. Ed.* **2012**, *51*, 6369–6372.
[18] J. Wu, Y. Zou, C. Li, W. Sicking, I. Piantanida, T. Yi, C. Schmuck, *J. Am. Chem. Soc.* **2012**, *134*, 1958–1961.
[19] K. Onizuka, Y. Taniguchi, S. Sasaki, *Bioconjugate Chem.* **2009**, *20*, 799–803.
[20] Y. Taniguchi, R. Kawaguchi, S. Sasaki, *J. Am. Chem. Soc.* **2011**, *133*, 7272–7275.
[21] N. Tabatadze, C. Tomas, R. McGonigal, B. Lin, A. Schook, A. Routtenberg, *Hippocampus* **2012**, *22*, 1228–1241.
[22] S.-H. Fujishima, R. Yasui, T. Miki, A. Ojida, I. Hamachi, *J. Am. Chem. Soc.* **2012**, *134*, 3961–3964.
[23] P. Arslan, A. Jyo, T. Ihara, *Org. Biomol. Chem.* **2010**, *8*, 4843–4848.
[24] M. Mukae, T. Ihara, M. Tabara, A. Jyo, *Org. Biomol. Chem.* **2009**, *7*, 1349–1354.
[25] T. Ihara, T. Fujii, M. Mukae, Y. Kitamura, A. Jyo, *J. Am. Chem. Soc.* **2004**, *126*, 8880–8881.
[26] T. Ihara, Y. Kitamura, Y. Tsujimura, A. Jyo, *Anal. Sci.* **2011**, *27*, 585–590.
[27] Y. Kitamura, T. Ihara, Y. Tsujimura, Y. Osawa, D. Sasahara, M. Yamamoto, K. Okada, M. Tazaki, A. Jyo, *J. Inorg. Biochem.* **2008**, *102*, 1921–1931.
[28] T. Ihara, T. Wasano, R. Nakatake, P. Arslan, A. Futamura, A. Jyo, *Chem. Commun.* **2011**, *47*, 12388–12390.
[29] T. Ogoshi, A. Harada, *Sensors* **2008**, *8*, 4961–4982.
[30] A. Ueno, S. Minato, I. Suzuki, M. Fukushima, M. Ohkubo, T. Osa, F. Hamada, K. Murai, *Chem. Lett.* **1990**, *19*, 605–608.
[31] R. Corradini, A. Dossena, R. Marchelli, A. Panagia, G. Sartor, M. Saviano, A. Lombardi, V. Pavone, *Chem. Eur. J.* **1996**, *2*, 373–381.

[32] *Molecular encapsulation: Organic reactions in constrained systems* (Eds.: U. H. Brinker, J.-L. Mieusset), Wiley, Chichester, **2011**.
[33] A. Kuzuya, T. Ohnishi, T. Wasano, S. Nagaoka, J. Sumaoka, T. Ihara, A. Jyo, M. Komiyama, *Bioconjugate Chem.* **2009**, *20*, 1643–1649.
[34] H. Takakusa, K. Kikuchi, Y. Urano, T. Higuchi, T. Nagano, *Anal. Chem.* **2001**, *73*, 939–942.
[35] H.-J. Schneider, A. K. Yatsimirsky, *Principles and Methods in Supramolecular Chemistry*, Wiley, Chichester, **2000**.
[36] T. Ihara, A. Uemura, A. Futamura, M. Shimizu, N. Baba, S. Nishizawa, N. Teramae, A. Jyo, *J. Am. Chem. Soc.* **2009**, *131*, 1386–1387.
[37] K. Yoshimoto, S. Nishizawa, M. Minagawa, N. Teramae, *J. Am. Chem. Soc.* **2003**, *125*, 8982–8983.
[38] B. Rajendar, A. Rajendran, Z. Ye, E. Kanai, Y. Sato, S. Nishizawa, M. Sikorski, N. Teramae, *Org. Biomol. Chem.* **2010**, *8*, 4949–4959.
[39] Y. Sato, Y. Zhang, T. Seino, T. Sugimoto, S. Nishizawa, N. Teramae, *Org. Biomol. Chem.* **2012**, *10*, 4003–4006.
[40] B. Rajendar, A. Rajendran, Y. Sato, S. Nishizawa, N. Teramae, *Bioorg. Med. Chem.* **2009**, *17*, 351–359.
[41] S. Miura, S. Nishizawa, A. Suzuki, Y. Fujimoto, K. Ono, Q. Gao, N. Teramae, *Chem. Eur. J.* **2011**, *17*, 14104–14110.
[42] A. Rajendran, C. Zhao, B. Rajendar, V. Thiagarajan, Y. Sato, S. Nishizawa, N. Teramae, *Biochim. Biophys. Acta Gen. Subj.* **2010**, *1800*, 599–610.
[43] C. Zhao, A. Rajendran, Q. Dai, S. Nishizawa, N. Teramae, *Anal. Sci.* **2008**, *24*, 693–695.
[44] W. A. Baase, W. C. Johnson, Jr., *Nucleic Acids Res.* **1979**, *6*, 797–814.
[45] C. R. Cantor, P. R. Schimmel, *Biophysical Chemistry: the Behavior of Biological Macromolecules*, W. H. Freeman, New York, **1980**.
[46] R. E. Dickerson, H. R. Drew, B. N. Conner, R. M. Wing, A. V. Fratini, M. L. Kopka, *Science* **1982**, *216*, 475.
[47] S. Neidle, *Oxford Handbook of Nucleic Acid Structure*, Oxford University Press, Oxford, **1999**.
[48] Y. Sato, T. Kageyama, S. Nishizawa, N. Teramae, *Anal. Sci.* **2013**, *29*, 15–19.
[49] Z. Ye, B. Rajendar, D. Qing, S. Nishizawa, N. Teramae, *Chem. Commun.* **2008**, 6588–6590.
[50] H. Dodziuk, *Cyclodextrins and Their Complexes.* Wiley-VCH, Weinheim. **2006**.
[51] F. S. Damos, R. Luz, A. A. Sabino, M. N. Eberlin, R. A. Pilli, L. T. Kubota, *J. Electroanal. Chem.* **2007**, *601*, 181–193.
[52] K. Fujita, T. Ueda, T. Imoto, I. Tabushi, N. Toh, T. Koga, *Bioorg. Chem.* **1982**, *11*, 108–114.
[53] C.-X. Wang, Y. Sato, M. Kudo, S. Nishizawa, N. Teramae, *Chem. Eur. J.* **2012**, *18*, 9481–9484.
[54] T. Russ, W. Ried, F. Ullrich, E. Mutschler, *Arch. Pharm.* **1992**, *325*, 761–767.

Received: March 14, 2013
Published online: July 2, 2013

Journal of Controlled Release 170 (2013) 469–476

Contents lists available at ScienceDirect

Journal of Controlled Release

journal homepage: www.elsevier.com/locate/jconrel

GENE DELIVERY

Stabilization of cancer-specific gene carrier via hydrophobic interaction for a clear-cut response to cancer signaling

Chan Woo Kim [a], Riki Toita [a], Jeong-Hun Kang [b], Kai Li [a], Eun Kyung Lee [a], Guo Xi Zhao [a], Daiki Funamoto [a], Takanobu Nobori [a], Yuta Nakamura [a], Takeshi Mori [a,c,d], Takuro Niidome [e], Yoshiki Katayama [a,c,d,f,*]

[a] Graduate School of Systems Life Sciences, Kyushu University, 744 Motooka, Nishi-ku, Fukuoka 819-0395, Japan
[b] Department of Biomedical Engineering, National Cerebral and Cardiovascular Center Research Institute, 5-7-1 Fujishiro-dai, Suita, Osaka 565-8565, Japan
[c] Department of Applied Chemistry, Faculty of Engineering, Kyushu University, 744 Motooka, Nishi-ku, Fukuoka 819-0395, Japan
[d] Center for Future Chemistry, Kyushu University, 744 Motooka, Nishi-ku, Fukuoka 819-0395, Japan
[e] Graduate School of Science and Technology, Kumamoto University, 2-39-1 Kurokami, Chuo-Ku, Kumamoto 860-8555, Japan
[f] Center for Advanced Medical Innovation, Kyushu University, 3-1-1 Maidashi, Higashi-ku, Fukuoka 812-8582, Japan

ARTICLE INFO

Article history:
Received 18 March 2013
Accepted 3 June 2013
Available online 18 June 2013

Keywords:
Gene delivery
Protein kinase
Transgene regulation
Hydrophobic interaction
Cancer

ABSTRACT

Here, we developed a new gene carrier, comprising a linear polyethylenimine (LPEI) grafted with a hydrophobically modified cationic peptide containing a long alkyl chain, for use in cancer-specific gene delivery. The cationic peptide is a substrate of protein kinase Cα (PKCα), which is known to be activated specifically in cancer cells. The hydrophobically modified LPEI-peptide conjugate (LPEI-C_{10}-peptide) could form a polyplex with DNA through electrostatic and hydrophobic interactions between the anionic DNA strands and the cationic peptide substrate. The hydrophobic modification of the peptide did not affect the reactivity of the peptide toward PKCα, while the polyplex showed improved intracellular uptake. Because of the efficient endosomal escape and enhanced stability, the polyplex significantly improved the transgene regulation responding to intracellular PKCα activity.

1. Introduction

Gene therapy has shown great promise for treating various diseases, such as cancers and other hereditary diseases. Although various approaches and efforts have been directed to the development of a proper gene delivery system, there remain significant obstacles to realizing an effective delivery of therapeutic genes to target sites without causing side effects as a result of undesirable gene expression in healthy cells or tissues [1–6]. To elude these barriers to such a gene delivery system, several functions such as gene packing, serum stability, cell internalization, cell-specific targeting, and facile regulation of gene expression should be endowed to the gene carriers.

As for the specific targeting of diseased cells, many kinds of stimuli-responsive carriers, which can respond to extracellular stimuli (e.g., tumor pH, enzymes, heat, light, and ultrasound) [7–10] and intracellular stimuli (e.g., endosomal pH, redox potential, and glutathione) [11–16], have been reported to achieve a more safe and effective drug or gene delivery system. On the other hand, we have developed another type of stimuli-responsive gene carrier that can respond to malfunctioning intracellular signaling in diseased cells. These gene carriers are composed of a hydrophilic polymeric main chain grafted with a cationic peptide which is a substrate of protein kinases activated specifically in the diseased cells. These carriers form a polyplex with anionic plasmid (pDNA) through electrostatic interaction between the anionic DNA strand and the cationic peptide, and the gene expression is effectively suppressed in the polyplex form. Once the polyplex is introduced into diseased cells, phosphorylation of the substrate peptide is conducted by protein kinases specifically targeting the diseased cells, which leads to dissociation of the polyplex for gene expression because of a decrease of the cationic charge of the grafted peptide. We have previously reported gene carriers that respond to hyper activation of intracellular protein kinases, such as IκB kinase β, protein kinase A, Rho-associated coiled-coil kinase, and protein kinase Cα (PKCα) [6,17–22].

Recently, we have developed a PKCα-responsive gene carrier in the form of a linear polyethylenimine (LPEI)–peptide conjugate [6], which showed quite high gene expression both *in vitro* and *in vivo* through responding to abnormally activated PKCα in cancer cells [23–27]. The quite sensitive response of the polyplex to PKCα results from efficient endosomal escape and tighter polyplex formation through densely grafted peptides. However, to enable intravenous administration of the gene carrier, the polyplex still needs further stabilization [6].

To stabilize polyplexes, many research groups have introduced hydrophobic interactions into the polyplex. Such hydrophobic interactions

* Corresponding author at: Department of Applied Chemistry, Faculty of Engineering, Kyushu University, 744 Motooka, Nishi-ku, Fukuoka 819-0395, Japan. Tel./fax: +81 92 802 2849.
E-mail address: ykatatcm@mail.cstm.kyushu-u.ac.jp (Y. Katayama).

0168-3659/$ – see front matter © 2013 Elsevier B.V. All rights reserved.
http://dx.doi.org/10.1016/j.jconrel.2013.06.011

are known to be enhanced in high ionic strength conditions, including physiological saline conditions, where electrostatic interaction is weakened [28–32]. Thus, here we designed a new gene carrier to stabilize the polyplex through hydrophobic interaction (Fig. 1). The carrier comprises a long alkyl spacer between the LPEI main chain and the peptide. This simple modification was found to effectively stabilize the polyplex, thereby leading to significantly improved PKCα-responsive gene expression.

2. Materials and methods

2.1. Materials

Rink Amide AM resin LL (100–200 mesh, amine density of 0.48 mmol/g) and all Fmoc-protected amino acids were obtained from Novabiochem, Merck (Tokyo, Japan). 1-hydroxybenzotriazole hydrate (HOBt·H2O), O-(benzotriazol-1-yl)-*N*,*N*,*N*′,*N*′-tetramethyluronium hexafluorophosphate (HBTU), diisopropylethylamine (DIPEA), dichloromethane (DCM), 1-methyl-2-pyrrolidone (NMP), and piperidine were purchased from Watanabe Chemical (Hiroshima, Japan). *N*,*N*-dimethylformamide (DMF) was purchased from Kanto Chemical (Tokyo, Japan). Sodium ascorbate, copper (II) sulfate pentahydrate, sodium azide, pyridine, dimethyl sulfoxide (DMSO), and ethanol were purchased from Wako Pure Chemicals (Osaka, Japan). 11-Bromoundecanoic acid, 5-chloro-1-pentyne, and 1,8-diazabicyclo[5,4,0]-7-undecene (DBU) were purchased from Tokyo Kasei Industry (Tokyo, Japan). Linear polyethylenimine (LPEI; Mw = 25,000) was purchased from Polysciences, Inc. (Warrington, PA, USA). All reagents were used without further purification.

2.2. Plasmid DNA

A plasmid DNA, pCMV-luc2, containing a firefly luciferase cDNA fragment driven by a CMV promoter was prepared as follows. A firefly luciferase cDNA fragment was obtained from the pGL4.10[luc2] vector (Promega, WI, USA) by *Hind*III and *Xba*I. This fragment was inserted into the pcDNA3 vector (Invitrogen, CA, USA). The resulting pDNA was amplified in the *Escherichia coli* strain DH5a, isolated, and then purified using a Qiagen Plasmid Mega Kit (Qiagen, CA, USA).

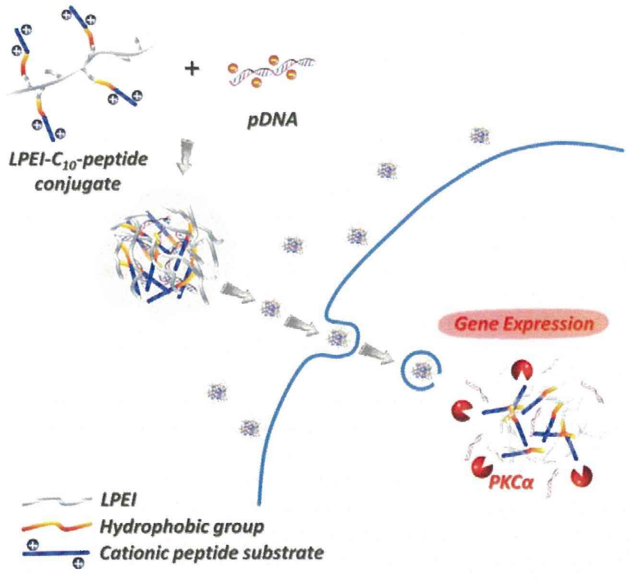

Fig. 1. Concept of a polyplex stabilized by hydrophobic interaction for application in cancer-specific gene expression. The LPEI-C_{10}-peptide conjugate forms stable polyplexes with pDNA through electrostatic interactions between the anionic DNA strands and the cationic peptide substrate moieties, as well as through an additional hydrophobic interaction. Despite the enhanced stability of the polyplexes, the polyplexes were dissociated specifically in cancer cells responding to the phosphorylation reaction by PKCα.

2.3. Synthesis of hydrophobically modified azido PKCα-specific peptide substrate

The peptide, FKKQGSFAKK, was prepared by standard Fmoc-chemistry using the Rink Amide AM resin LL (100–200 mesh, amine density of 0.48 mmol/g), DIPEA as a base, HOBt/HBTU as coupling reagents, and a 20% solution of piperidine in DMF for deprotection of the Fmoc group as described previously. To modify the hydrophobic groups on the peptide substrate, 11-azidoundecanoic acid was synthesized from 11-bromoundecanoic acid by addition of two equivalents of sodium azide for 1 day at room temperature in 1:1 DMF/DMSO solution. 11-Azidoundecanoic acid was then reacted with the *N*-terminus of the peptide in the presence of the coupling reagents. After completion of the reaction, the peptide was cleaved from the resin and was purified by reverse-phase liquid chromatography. The obtained peptide substrate, N_3-$(CH_2)_{10}$-CO-FKKQGSFAKK-NH_2 [C_{10}(S)] was identified by MALDI-TOF-MS. N_3-$(CH_2)_{10}$-CO-FKKQGAFAKK-NH_2 [C_{10}(A)] as a control peptide substrate was synthesized in the same manner.

2.4. Synthesis of hydrophobically modified LPEI-peptide conjugate

Hydrophobically modified LPEI-peptide conjugates were synthesized by following a two-step synthetic procedure as described previously [6]. LPEI was dissolved in dry DMSO (30 mL) followed by addition of pyridine, 1,8-diazabicyclo[5,4,0]-7-undecene (DBU), and 5-chloro-1-pentyne. After the reaction, DMSO was partially evaporated under reduced pressure. The residue was diluted in methanol and dialyzed by using a dialysis membrane bag (MW cut off, 10,000) against methanol, then 0.05 N HCl, and finally water. The obtained polymer (LPEI-pentyne) was mixed with the azido peptide substrate [C_{10}(S) or C_{10}(A)], copper (II) sulfate pentahydrate, and sodium ascorbate in 800 μL of water/ethanol (1/1 = v/v) and the mixture was maintained at room temperature with continuous stirring for one day. After the reaction, the crude product was dialyzed against 0.05 N HCl and then water by using a dialysis membrane bag (MW cut off, 10,000), followed by freeze-drying to obtain the conjugate, LPEI-C_{10}(S) and LPEI-C_{10}(A). The contents of the peptide substrate were determined by ^{1}H NMR spectra. LPEI-C_2(S) and LPEI-C_2(A) were synthesized in the same manner.

2.5. Phosphorylation assay of the azido peptide substrate

The phosphorylation of C_2(S) and C_{10}(S) responding to PKCα was carried out in 100 μL buffer [10 mM HEPES, 10 mM $MgCl_2$, 0.5 mM $CaCl_2$, 2.0 μg/mL diacylglycerol (DAG), 2.5 μg/mL phosphatidylserine (PS), and 200 μM ATP] containing 30 μM azido peptide substrate and 0.1 μg/mL PKCα. The phosphorylation was allowed to proceed for 1 h at 37 °C and then the resulting solutions were analyzed by MALDI-TOF-MS [33].

2.6. Phosphorylation assay of polymer using a coupled enzyme assay

The phosphorylation profiles of LPEI-C_2(S/A) and LPEI-C_{10}(S/A) were examined using a coupled enzyme assay [21,34]. The reaction was performed in 20 mM HEPES buffer [200 μM ATP, 10 mM $MgCl_2$, 0.5 mM $CaCl_2$, 2.0 μg/mL DAG, 2.5 μg/mL PS, 0.3 mM nicotinamide adenine dinucleotide (NADH), 1 mM phosphoenolpyruvate, 10 U/μL LDH, and 4 U/μL pyruvate kinase] containing 30 μM polymer at 25 °C. Monitoring of NADH consumption was initiated by adding 1.1 ng/μL PKCα and detected with a UV/Vis spectrophotometer (UV-2550; Shimadzu, Tokyo, Japan) equipped with an SPR-8 temperature controller (Shimadzu) at 340 nm.

2.7. Agarose gel electrophoresis

Polyplexes at various *N/P* ratios were prepared with pDNA (0.2 μg) and different concentrations of polymer in 10 μL HEPES buffer (100 mM, pH 7.3) for 15 min at room temperature. The formation of the polyplexes was analyzed by 1% agarose gel electrophoresis at 100 V for 30 min.

2.8. Ethidium bromide (EtBr) exclusion assay

Five microliters of pDNA (0.1 μg/μL) was prepared with 1.25 μL of EtBr (0.1 μg/μL) for 5 min. Polyplexes at various *N/P* ratios were prepared by adding different concentrations of polymer for 15 min and the volume of each sample was adjusted to 100 μL with 10 mM HEPES. Assays were performed at room temperature in the dark. Fluorescence measurements of each sample were performed at 25 °C using a multilabel counter ARVO (Wallac Incorporated, Turku, Finland). Excitation and emission wavelengths were 530 nm and 590 nm, respectively. The relative fluorescence intensity (RFI) was determined by using the following equation: $RFI = (F_{obs} - F_e) / (F_0 - F_e)$, where F_{obs}, F_e and F_0 are the fluorescence intensities of the polyplex at each *N/P* ratio, back ground (EtBr only), and naked pDNA, respectively.

2.9. Dynamic light scattering (DLS) measurement

Polyplexes at various *N/P* ratios were prepared with pDNA and different concentrations of polymer by mixing at room temperature for 20 min. The final concentration of pDNA was adjusted to 20 μg/mL in 10 mM HEPES buffer or Dulbecco's modified Eagle's medium (DMEM) (Gibco Invitrogen Co., Grand Island, NY, USA) containing 10% fetal bovine serum (FBS). The diameters of the polymer/pDNA polyplexes were measured by a Zetasizer (Malvern Instruments, Worcestershire, UK) with the He/Ne laser at a detection angle of 173° at 25 °C.

2.10. Cell culture

A549 cells were cultured in DMEM containing 10% FBS, 100 U/mL penicillin, 100 μg/mL streptomycin, and 0.25 μg/mL amphotericin B (all from Gibco). The cell was harvested in a humidified atmosphere containing 5% CO_2 and 95% air at 37 °C.

2.11. Cellular uptake of polyplex

The pDNA was fluorescently labeled with the intercalating nucleic acid dye YOYO-1 iodide (diluted from 1 mM stock solution in DMSO, Molecular Probes) for uptake analysis [35]. 500 μL of pDNA (0.1 mg/mL) was combined with 100 μL of TAE buffer and 400 μL of 10 μL YOYO-1 in TE buffer in a microcentrifuge tube. The solution was mixed for at least 1 h at room temperature in the dark wrapped in foil and stored at −20 °C.

200 μL aliquots of growing A549 cell suspension (30,000 cells) were seeded into a 48-well plate in DMEM containing 10% FBS. After incubation for 24 h, the medium in each well was replaced with Opti-MEM (Gibco) containing the YOYO-1-labeled pDNA/polymer polyplex at the *N/P* ratio 7, and incubated for 2 h. Estimation of cellular uptake was conducted by a Tali™ Image-Based Cytometer (Invitrogen).

2.12. Confocal laser scanning microscopy (CLSM)

A549 cells were plated at a density of 1×10^5 in 35-mm glass bottom dishes (Matsunami, Osaka, Japan) at 37 °C in 1 mL of DMEM containing 10% FBS for 24 h. pDNA was labeled with tetramethylrhodamine (TAMRA) by using a Label-IT reagent (Mirus, WI, USA) (labeling efficiency; 1 TAMRA/100 base pair). Polyplexes at the *N/P* ratio of 7 were prepared with TAMRA-labeled pDNA (2 μg) and polymer for 20 min at room temperature. The medium was replaced with Opti-MEM containing pDNA/polymer polyplexes. After incubation for 6 h, the medium was changed to DMEM containing 10% FBS, and the cells were further incubated for 18 h. Polyplexes were observed by CLSM (ZEISS LSM 700, Carl Zeiss, Oberlochen, Germarny) equipped with a Plan-Apochromat 63×/1.40 Oil Ph3 M27 objective after staining acidic late endosomes and lysosomes with LysoTracker Green for 1 h and nuclei with Hoechst 33342 (Molecular Probes, Eugene, OR) for 15 min before each observation.

2.13. Cytotoxicity of polyplex

Cell viability was assessed using a cell counting kit containing 4-[3-(2-methoxy-4-nitrophenyl)-2-(4-nitrophenyl)-2H-5-tetrazolio]-1,3-benzene disulfonate sodium salt (WST-8) (Dojindo Laboratories, Kumamoto, Japan). Briefly, 2×10^3 cells were seeded into a 96-well plate and cultured for 24 h at 37 °C in a 5% CO_2 incubator. The medium in each well was replaced with 100 μL of fresh medium containing polyplexes at various *N/P* ratios (0 to 10) with pDNA (0.5 μg/well) and different concentrations of polymer (7.1 to 26 μg/mL). After incubation for 24 h, the medium was replaced with 100 μL of fresh medium containing WST-8. The cells were incubated for a further 2 h, before measurement of the absorbance at 440 nm. The cell viability (%) was calculated by normalizing the absorbance of the treated cells to that of the untreated control cells. This assay was performed in triplicate.

2.14. Transfection study

A549 cells were plated at a density of 3×10^4 in 48-well plates at 37 °C in DMEM containing 10% FBS for 24 h. Polyplexes at various *N/P* ratios were prepared with pDNA (1 μg) and different concentrations of polymer for 20 min at room temperature. The medium in each well was replaced with Opti-MEM containing pDNA/polymer polyplexes at various *N/P* ratios. After incubation for 4 h, the medium was changed

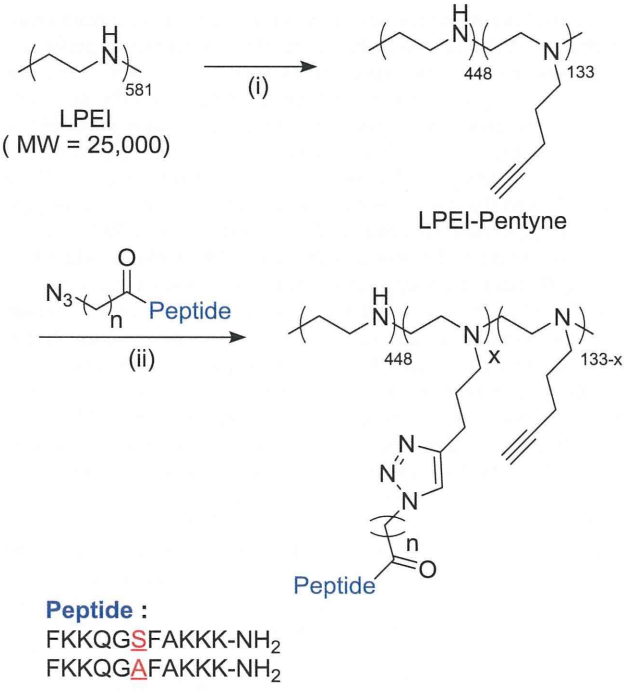

Scheme 1. Synthetic scheme for preparing hydrophobically modified LPEI-peptide conjugates.[a]. [a]Reagents and conditions: (i) 5-chloro-1-pentyne, DBU, and dry DMSO at 50 °C; (ii) *N*-terminus azido-peptide, copper(II) pentahydrate, sodium ascorbate, and H_2O/ethanol = 1/1 at room temperature.

to DMEM containing 10% FBS, and the cells were further incubated for 20 h. The cultured cells were then scraped and lysed in 100 μL of lysis buffer (20 mM Tris–HCl, pH 7.4, 0.05% Triton-X 100, and 2 mM EDTA). A 10-μL aliquot of the lysate solution was used for measuring chemiluminescence in a MiniLumat LB 9506 (EG & G Berthold, Wildbad, Germany) directly after mixing with 40 μL of the luciferin substrate. The results are presented as relative luminescence units (RLU)/mg total protein.

3. Results and discussion

3.1. Reactivity of hydrophobically modified peptide substrate to PKCα

We previously used a propionic acid linker for synthesizing azide groups modification on a terminus of the peptide substrate [6]. Here we exchanged the linker for the much more hydrophobic undecanoic acid with the aim of achieving further stabilization of the polyplex as shown in Scheme 1. We selected the *N*-terminus of the peptide for the modification of the azide group, because we previously found that chemical modification of the *N*-terminus did not affect the overall reactivity of the peptide. In contrast, chemical modification of the *C*-terminus of the peptide severely reduced the reactivity of the peptide. The azide group was modified on the *N*-terminus of the peptide in the last step of a solid phase peptide synthesis. Then, we assessed whether the reactivity of the resulting peptide, $C_{10}(S)$ [N_3-$(CH_2)_{10}$-CO-FKKQGSFAKKK-NH_2], toward PKCα is affected by the hydrophobic modification by using MALDI-TOF-MS. As shown in Fig. 2, the phosphorylation of $C_{10}(S)$ by PKCα was somewhat slower than that of $C_2(S)$. However, after 30 min, the phosphorylation reaction of both $C_2(S)$ and $C_{10}(S)$ was almost saturated, indicating that the effect of the modification of the hydrophobic long alkyl chain on the reactivity of the peptide substrate to PKCα was not significant.

3.2. Reactivity of hydrophobically modified LPEI-peptide polymer to PKCα

The modification of the peptide substrates on LPEI as a main chain, which is one of the most well-characterized gene carriers, was performed via a two-step synthetic procedure as shown in Scheme 1 [6]. The contents of the peptide substrate were calculated from the peak area ratio comparison between the protons of the phenyl groups in the peptide substrate (−CH−, δ = 7.13 ppm) and the methylene protons of LPEI (−CH_2−, δ = 2.85 ppm) by ^{1}H NMR spectra in D_2O (Fig. S1). These results showed that the contents of the peptide substrate in LPEI-$C_{10}(S)$ and LPEI-$C_{10}(A)$ were 10.8 mol% and 11.0 mol%, respectively (Table 1).

The reactivity of the peptide substrate to PKCα after modification of the LPEI main chain was evaluated using a coupled enzyme assay [36]. The phosphorylation of the peptide substrate was identified from the decrease of absorbance at 340 nm resulting from NADH reduction which is caused by the consumption of ATP during the phosphorylation reaction of the peptide substrate. As shown in Fig. 3, LPEI-$C_{10}(A)$ showed no change in the absorption, while LPEI-$C_{10}(S)$ showed steep decrease of the absorption resulting from the phosphorylation of the grafted peptide. Although the reaction rate of LPEI-$C_{10}(S)$ is slower than that of the original peptide $C_{10}(S)$, the reaction rate of LPEI-$C_{10}(S)$ is surprisingly identical to that of LPEI-$C_2(S)$. Thus, the effect of the long alkyl chain on the reactivity of the $C_{10}(S)$ peptide disappeared when the $C_{10}(S)$ peptide was modified onto the LPEI main chain. This is probably because the hydrophobic alkyl chain is hidden behind the peptide after modification onto the LPEI backbone.

3.3. pDNA condensation ability of hydrophobically modified LPEI-peptide polymer

To verify the stoichiometry of the binding of the polymers to pDNA, an agarose gel electrophoresis assay was conducted with varying *N/P*

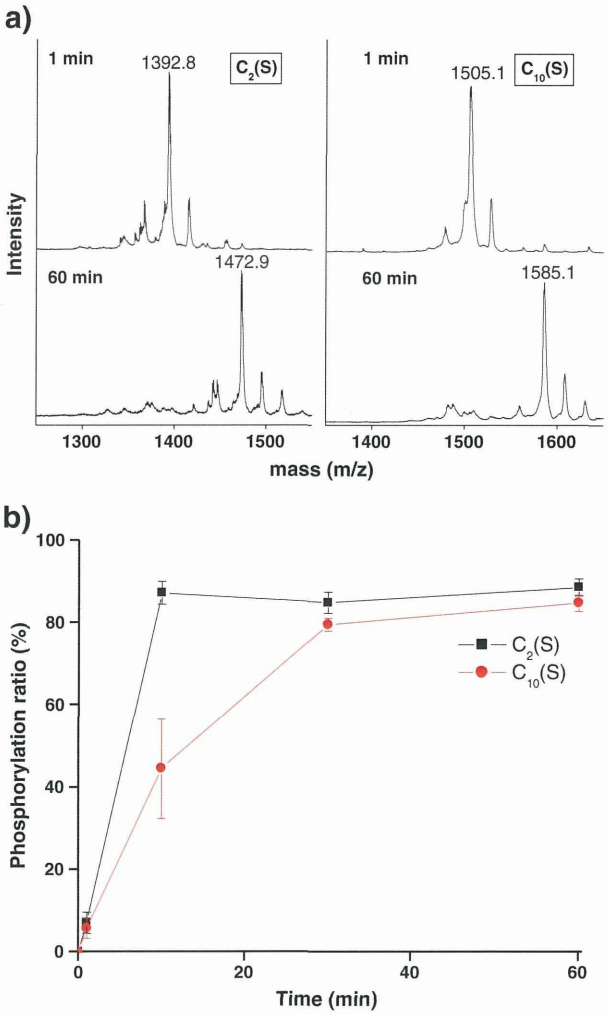

Fig. 2. (a) Phosphorylation reactions of $C_2(S)$ and $C_{10}(S)$ in the presence of PKCα at 37 °C. (b) Time-dependent changes of the ratio of phosphorylation reactions. Phosphorylation ratios were identified by MALDI-TOF-MS analysis (n = 3).

ratios. The electrophoretic patterns for both LPEI-$C_2(S)$ and LPEI-$C_{10}(S)$ showed that free pDNA completely disappeared from the same *N/P* ratio of 2 (Fig. 4a). Thus, the long alkyl chain of LPEI-$C_{10}(S)$ seems not to interrupt the polyplex formation.

The stoichiometry in the polyplex formation was also verified by using an EtBr exclusion assay. EtBr produces a high fluorescence on interaction with nucleobases, whereas the fluorescence intensity is significantly suppressed by the inhibition of the intercalating processes of EtBr to DNA caused by the polyplex formation and condensation [37]. Thus, the distinct fluorescence intensity of intercalated EtBr is used to estimate the stoichiometry of the polyplex formation. As shown in Fig. 4b, all four curves are almost superimposable and the relative fluorescence intensity (RFI) reached a plateau when the *N/P* ratio was 3. This result again shows that the long alkyl chain does not disturb the polyplex formation. We previously found that, in LPEI-$C_2(S)$, the cationic charges of the peptide substrate mainly contribute to the polyplex formation while the charges of the LPEI main chain show negligible contribution to the condensation of pDNA probably because of shielding of the cationic charges on the LPEI backbone by the bulky pentyne group [6]. The identical curves of LPEI-$C_{10}(S)$ to LPEI-$C_2(S)$ showed that the cationic charges of the peptide also contributed mainly to the polyplex formation in the case of LPEI-$C_{10}(S)$. It is noteworthy that the anionic pDNA selectively binds to

Table 1
Molecular parameters of carriers.

Samples	n, alkyl chain length	Peptide sequence	Peptide content[a]/mol%	Peptide no./chain	M_w[b]/10^4 g/mol
LPEI-C_2(S)	2	-FKKQGSFAKKK-NH_2	10.9	63	12.1
LPEI-C_2(A)	2	-FKKQGAFAKKK-NH_2	8.1	47	9.8
LPEI-C_{10}(S)	10	-FKKQGSFAKKK-NH_2	10.8	62	12.7
LPEI-C_{10}(A)	10	-FKKQGAFAKKK-NH_2	11.0	63	12.8

[a] Determined by ^{1}H NMR spectra.
[b] Calculated from peptide and pentyne contents and M_w of the parent LPEI.

the cationic peptide of the carriers. This property is crucial for our transgene regulation system, which is specifically responsive to intracellular PKCα via phosphorylation reaction of the peptide substrate.

The size and size distribution of the polyplexes of LPEI-C_{10}(S) to LPEI-C_2(S) were investigated in 10 mM HEPES buffer at the *N/P* ratio of 7 and 10 (Table S1). The size of the polyplexes both of LPEI-C_{10}(S) to LPEI-C_2(S) were around 100 nm irrespective of the *N/P* ratios. The polydispersity index (PDI) of the both polyplexes was less than 0.21, which shows relatively narrow size distribution of these polyplexes. We then examined the stability of the polyplexes against mixing with DMEM containing 10% FBS (Fig. 2). The diameter of the polyplex from LPEI-C_{10}(S) is as stable as that of LPEI-C_2(S). No interparticle aggregation was observed in both polyplexes when mixing with the medium. This result may indicate that the hydrophobic alkyl groups are not exposed to the surface of the polyplexes to induce interparticle aggregation.

3.4. Cytotoxicity and cellular uptake of hydrophobically modified polyplexes

The cytotoxicity of each of the polyplexes was evaluated prior to *in vitro* studies. As shown in Fig. 5, both LPEI-C_2(S) and LPEI-C_2(A) showed weak cytotoxicity at N/P of 10, while the alkyl chain modified conjugates, LPEI-C_{10}(S) and LPEI-C_{10}(A) showed no detectable cytotoxicity. Thus, the hydrophobic alkyl modification somewhat reduced the cytotoxicity of the polymers.

To gain a better insight into the effect of an additional hydrophobic interaction, the cellular uptake of the polyplexes was monitored by using pDNA labeled with YOYO-1. As shown in Fig. 6, the uptake of the LPEI-C_{10}(S) polyplex was higher than the LPEI-C_2(S) polyplex. The introduction of hydrophobic groups onto the polymer improved the intracellular uptake of the polyplexes probably because of the enhanced stability in the medium, which includes high concentrations of organic and inorganic salts and other ingredients. The enhanced stability of the polyplex will work to avoid undesirable transgene expression without phosphorylation.

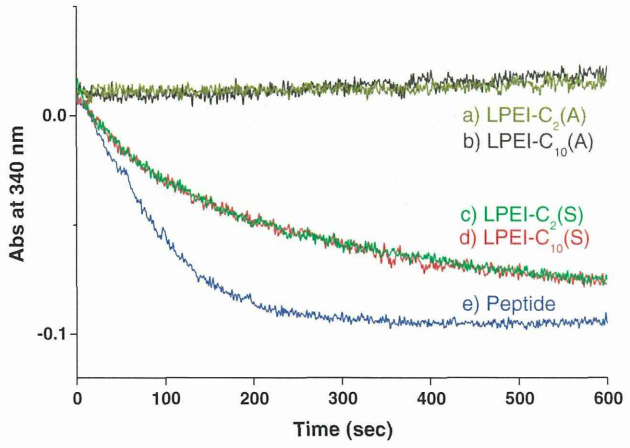

Fig. 3. Reactivity of LPEI-peptide conjugates and original peptide (H-FKKQGSFAKKK-NH_2) toward PKCα monitored by a coupled enzyme assay. The phosphorylation reaction was identified from the decrease of absorbance at 340 nm by NADH reduction.

3.5. Intracellular trafficking of polyplexes

The intracellular trafficking of LPEI-C_2(S) and LPEI-C_{10}(S) polyplexes was monitored by CLSM. We used here pDNA labeled with TAMRA and stained nuclei and late endosomes/lysosomes with Hoechst 33342 and LysoTracker Green, respectively. As shown in Fig. 7, the fluorescent dots resulting from pDNA complexed with both LPEI-C_2(S) and LPEI-C_{10}(S)

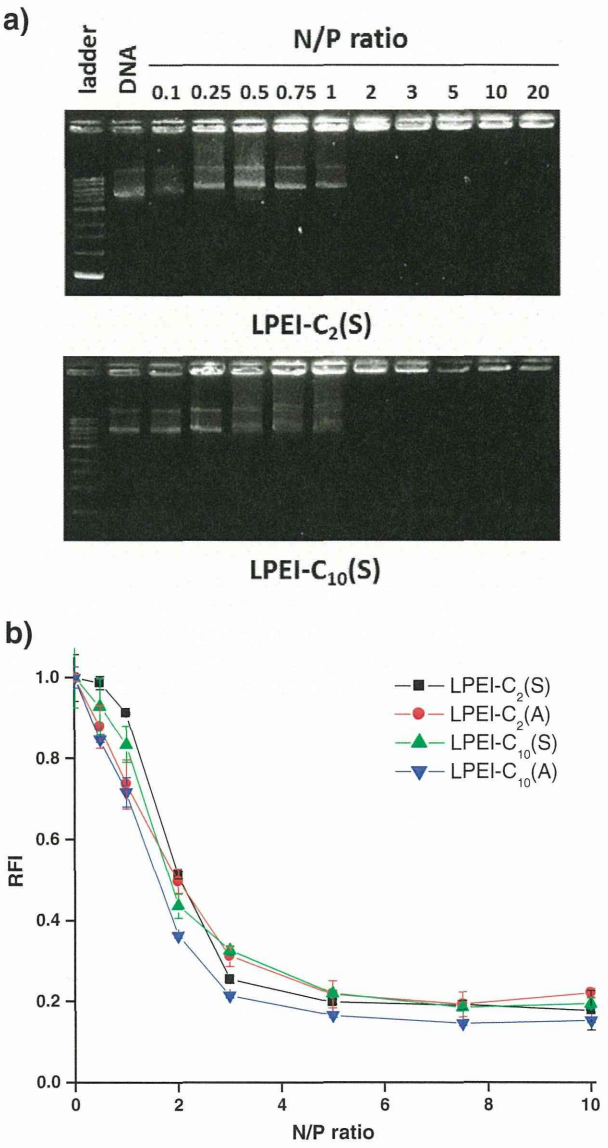

Fig. 4. Polyplex formation of the LPEI-peptide conjugate with pDNA. (a) Agarose gel electrophoresis of the conjugates and pDNA with varying *N/P* ratios. (b) EtBr exclusion assay of conjugates was performed by monitoring the distinct fluorescence intensity of intercalated EtBr (n = 3).

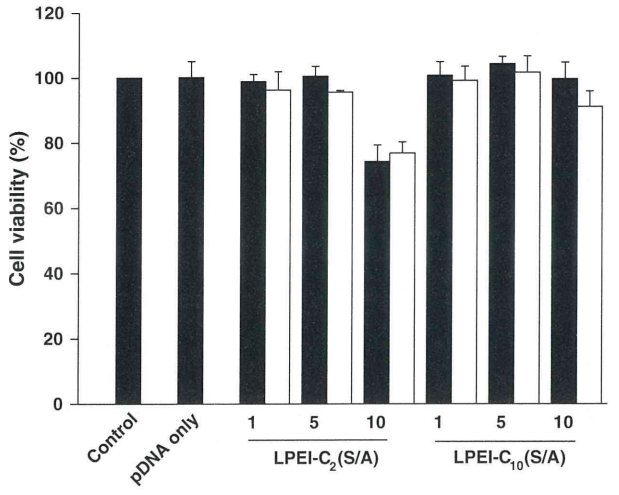

Fig. 5. Cytotoxicity of polyplexes of LPEI-peptide conjugates for A549 cells (n = 3). LPEI-C_2(S) and LPEI-C_{10}(S) are shown as filled bars, and LPEI-C_2(A) and LPEI-C_{10}(A) are shown as open bars.

were observed in the cytoplasm with yellow and red, which results from the polyplex existing in the endosome and in the cytosol, respectively. In contrast, much smaller numbers of fluorescent dots were detected in the polyplex of LPEI-pentyne because of the weak complexation with pDNA [6]. These results indicated that LPEI-C_2(S) and LPEI-C_{10}(S) formed stable polyplexes with the grafted peptide and efficiently taken up by cells via endocytosis. The large number of red fluorescent dots of the polyplexes suggested that the buffering capacity of the LPEI main chain of LPEI-C_2(S) and LPEI-C_{10}(S) leads to escape from the endosome by the proton sponge effect [3].

3.6. Effect of hydrophobic interaction on regulation of transgene expression

The transgene regulation of the polyplexes was evaluated using luciferase-encoding pDNA in A549 cells, in which intracellular PKCα is known to be hyperactivated [20,33,34]. As shown in Fig. 8, the gene expression of negative control polyplexes [LPEI-C_2(A) and LPEI-C_{10}(A)] was kept at a low level ($<10^7$ RLU/mg protein), while the LPEI-C_2(S) and LPEI-C_{10}(S) polyplexes showed much higher gene expression, irrespective of the *N/P* ratios. This result clearly showed a suppression of gene expression in the negative control polyplexes and the PKCα-responsive gene expression in LPEI-C_2(S) and LPEI-C_{10}(S) polyplexes.

As for the effect of the alkyl chains, the LPEI-C_{10}(S) polyplex showed a more than ten times higher gene expression than the LPEI-C_2(S) polyplex at both the *N/P* ratios of 5 and 7. The higher gene expression in LPEI-C_{10}(S) should result from the improved cellular uptake in the transfection medium, which includes a high concentration of organic and inorganic salts as clarified in Fig. 6. Despite the improved cellular uptake in the LPEI-C_{10}(S) polyplex, the gene expression of the negative control polyplex of LPEI-C_{10}(A) which also has the long alkyl chain showed a level of suppressed gene expression that was low as that of

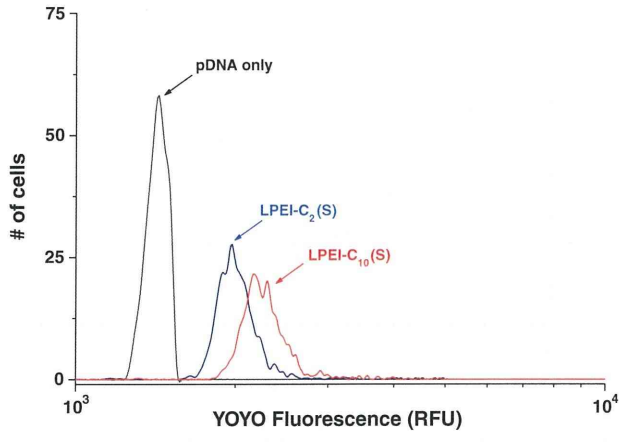

Fig. 6. Cellular uptake of LPEI-C_2(S) and LPEI-C_{10}(S) polyplexes with YOYO-1-labeled pDNA in A549 cells. The *N/P* ratio of the polyplexes of the polymers was 7.

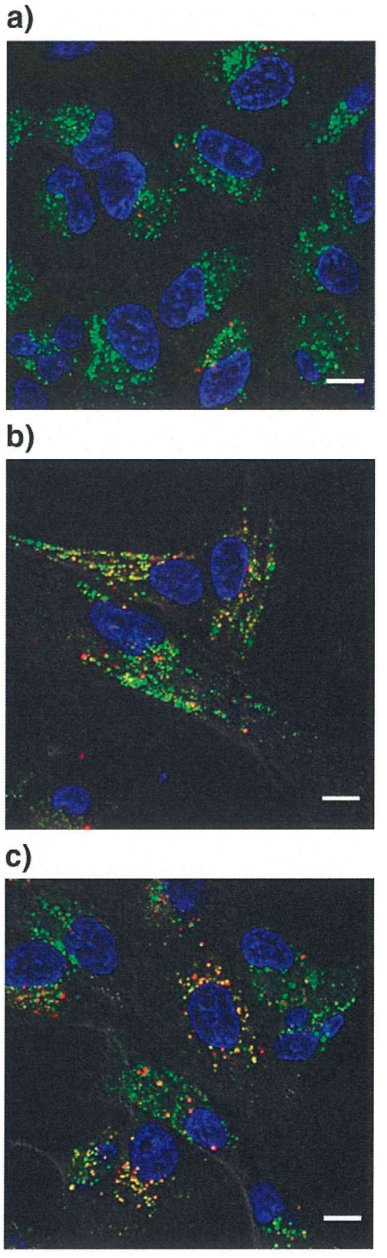

Fig. 7. Intracellular distribution of (a) LPEI-pentyne, (b) LPEI-C_2(S), and (c) LPEI-C_{10}(S) polyplexes in A549 cells. pDNA was labeled with TAMRA (red). Late endosomes/lysosomes and the nuclei were stained with LysoTracker Green (green) and Hoechst 33342 (blue), respectively. The scale bar represents 20 μm.